Am J Transl Res 2023;15(2):817-833
www.ajtr.org /ISSN:1943-8141/AJTR0147707

Original Article

ISG15 is a potential therapeutic target for osteosarcoma: a comprehensive analysis based on bioinformatics and in vitro experiments

Yedan Liao[1,2*], Xueqi Zhang[2*], Jiadai Tang[2], Fengdi Hu[1], Dongqi Li[3], Hongli Song[2], Jiaojiao Chen[2], Jiangyan Guo[4], Rong Li[1,2], Yanping Lin[1,2], Lin Xie[1]

[1]Department of Gastrointestinal Oncology, The Third Affiliated Hospital of Kunming Medical University (Yunnan Cancer Hospital, Yunnan Cancer Center), Kunming, Yunnan, China; [2]Graduate School, Kunming Medical University, Kunming, Yunnan, China; [3]Bone and Soft Tissue Tumors Research Center of Yunnan Province, Department of Orthopaedics, The Third Affiliated Hospital of Kunming Medical University (Yunnan Cancer Hospital, Yunnan Cancer Center), Kunming, Yunnan, China; [4]Department of Clinical Pathology, The Third Affiliated Hospital of Kunming Medical University (Yunnan Cancer Hospital, Yunnan Cancer Center), Kunming, Yunnan, China. [*]Equal contributors.

Received November 12, 2022; Accepted January 6, 2023; Epub February 15, 2023; Published February 28, 2023

Abstract: Background: The expression of aberrant interferon-stimulated gene 15 (ISG15) is connected with various human diseases, including cancer. ISG15 is involved in tumor formation and metastasis. However, its role in osteosarcoma is uncertain. Methods: ISG15 expression in pan-cancer from RNA Sequencing data were obtained from The Cancer Genome Atlas (TCGA) and Genotype Tissue Expression (GTEx) databases. The relationship between ISG15 expression and prognosis was assessed through TCGA clinical survival data. Immunohistochemistry (IHC) images of ISG15 were retrieved using the Human Protein Atlas to analyze the differences in selected normal and tumor tissues. Gene enrichment analysis and signaling pathway analysis were used to assess the potential role of ISG15 in sarcoma, and the correlation between ISG15 expressions and immune cell infiltration levels was estimated by immune infiltration analysis. The expression levels of ISG15 were assessed by qRT-PCR and IHC. Colony formation, wound healing assay and transwell assay were used to detect the effects of ISG15 on the biological behaviors of osteosarcoma cells. The correlation between ISG15 levels and CD8+/CD68+ cells was further examined by double-labeled immunofluorescence. The chemotactic effect of ISG15 on CD8+/CD68+ cells was demonstrated by chemotactic experiments and flow cytometry. Results: ISG15 was highly expressed in most cancers, while high ISG15 expression was significantly correlated with poor overall survival. Gene enrichment analysis in sarcoma suggested that antigen processing and presentation might be involved in the oncogenic mechanism of ISG15. Further immune infiltration analysis showed that high ISG15 expression might reflect the infiltration level of certain immune cells. Additionally, our verification showed that ISG15 was significantly related to the occurrence and metastasis of osteosarcoma, and knockdown of ISG15 significantly altered cell biological behavior, resulting in decreased proliferation, migration and invasion capabilities of osteosarcoma cells. The high expression of ISG15 in osteosarcoma tissue was associated with a high level of CD68+ immune cell infiltration while a low level of CD8+ T cell infiltration. CD68+ immune cells were recruited in vitro by overexpression of ISG15, which on the contrary could weaken the chemotaxis of CD8+ T cells. Conclusion: High ISG15 expression is an inherent feature of osteosarcoma and triggers tumorigenesis and metastasis by regulating tumor immunogenicity. ISG15 is expected to be the target of osteosarcoma treatment.

Keywords: ISG15, immune infiltration, biomarker, osteosarcoma metastasis, prognosis

Introduction

Osteosarcoma is a malignant osteogenic tumor that occurs more commonly in adolescents or children under the age of 20, accounting for approximately 55-60% of all malignant bone tumors [1]. With the combined application of neoadjuvant chemotherapy, surgery and adjuvant chemotherapy, the 5-year survival rate of the non-metastatic osteosarcoma has been significantly improved to 65-75% [2]. However, osteosarcoma has a high capacity for local infil-

tration and a propensity for distant metastases, resulting in the metastatic lesions detected at initial presentation in many patients, with the most common sites of metastasis being lung and bone [3]. Patients with metastatic or recurrent osteosarcoma have a poor prognosis, with an overall 5-year survival rate of only 10-30%, and little improvement has been made in survival over the past 30 years [4-7]. Therefore, the key to reducing osteosarcoma mortality and improving prognoses lies in studying its growth and metastasis.

As the first discovered ubiquitin-like protein, ISG15 has a highly homologous functional domain similar to ubiquitin at both the amino and carboxy ends and is one of the major effector proteins of type I interferons [8]. Despite the immense complexity of ISG15, increasing evidence suggests that ISG15 is involved in multiple key cellular processes, such as those involved in immune regulation, autophagy, protein translation, exosome secretion and DNA repair, underscoring the re-evaluation of ISG15 functional necessity [9]. ISG15 is involved in tumor formation and metastasis. Our previous research found that ISG15 was a significantly up-regulated hub protein in the network of metastatic osteosarcoma [10]. The microenvironment influences the pathogenesis of solid tumors and plays a vital role in some solid tumors [11]. Studies have shown that ISG15 plays a crucial role in the tumor microenvironment (TME) by enhancing cytokines of T-cell, B-cell and epithelial-cell lineages [12].

In our study, we systematically analyzed the expression levels and prognostic value of ISG15 across cancers. Further attention was given to the prognostic impact of ISG15 gene alterations, links between ISG15 expression and molecular pathways in sarcomas, and correlations of ISG15 with immune infiltration. Finally, we conducted a series of experiments at clinical and cellular levels to clarify the effect of ISG15 on osteosarcoma, and the possible mechanisms of its induction and promotion of osteosarcoma were comprehensively discussed.

Materials and methods

RNA sequencing (RNA-Seq) data collection and analysis

To evaluate ISG15 expression at a mRNA level in pan-cancer paired samples (tumor and normal tissues), we first downloaded data from The Cancer Genome Atlas (TCGA). Then, we analyzed the ISG15 expressions in unpaired samples through the TPM-formatted RNA-Seq data obtained from TCGA and Genotype Tissue Expression (GTEx). At last, R (version 3.6.3) was used for statistical analysis and visualization, and the R package (mainly ggplot2 [version 3.3.3]) was used for visualization.

Immunohistochemistry (IHC) image retrieval and analysis

IHC images of ISG15 protein expressions were retrieved from Human Protein Atlas (HPA) and used to assess the ISG15 expression differences in normal and tumor tissues.

Survival prognosis analysis

The R package "survival" (version 3.6) was used to obtain a KM survival curve plot of overall survival (OS) for ISG15. The cohort was divided into high and low expression groups by "0-50 vs. 50-100" or the division threshold value that minimizes the *P* value. Visualization was performed using "ggplot2".

Correlation and gene set enrichment analysis

Data were collected from TCGA for analysis of ISG15 mRNA with other associated genes in sarcoma. The top 100 genes that were most positively associated with ISG15 were selected for enrichment analysis to demonstrate the biological function of ISG15. The EnrichGO function "clusterProfiler" in the R package was used to perform gene ontology (GO) enrichment and included biological process (BP), cellular component (CC) and molecular function (MF). The enrichKEGG function in the R package "clusterProfiler" was used to perform Kyoto Encyclopedia of Genes and Genomes (KEGG) analysis.

Immune cell infiltration analysis

We used the single sample GSEA (ssGSEA) method package GSVA (version 1.34.0) [13] to comprehensively study the levels of tumor immune infiltration. Twenty-four immune cell markers were obtained from a previous study [14]. We used RNA-Seq data based on the level 3 HTSeq-FPKM format from the TCGA-SARC project dataset. The data were transformed into TPM format, subjected to log2 transforma-

tion, and then filtered to detect the effect of ISG15 expression on immune cell infiltration. The correlation between ISG15 expression and immune cells was explored by calculating *p* values using Spearman correlation analysis.

Validation experiments on clinical tissue samples

A total of 28 tumor tissue and 19 adjacent/normal tissue were obtained from patients undergoing osteosarcoma amputation or limb salvage surgery in the Yunnan Cancer Hospital. Among them, 19 tumor and 19 normal samples were paired. Besides, we collected the lung metastatic lesions of 5 patients among the 15 patients with lung metastasis, as well as relevant clinical information of the all included patients. Osteosarcoma diagnoses were confirmed by histopathology, and lung metastases were confirmed by imaging or pathology. The sample diameters were approximately 5-10 mm. They were immersed in RNAlater and stored in a freezer at -80°C for qRT-PCR experiments. For the IHC experiments, the sample were immersed in 4% paraformaldehyde and stored at room temperature. All specimens were made into 4 to 6-μm sections and immunohistochemically stained for ISG15 using the ready-to-use immunohistochemical MaxVision HRP kits (MXB Biotechnologies, Kit-5030). The human ISG15/UCRP antibody (R&D Systems, Monoclonal Mouse IgG2B Clone # 539442) was diluted at 1:100. For paraffin section double-labeled immunofluorescence experiments, the sections were dewaxed to water, after antigen retrieval with EDTA, circled with histochemical strokes (Servicebio, G6100), blocked with hydrogen peroxide and serum. Then, the corresponding antibodies were added in order for incubation (ISG15 Antibody, BOSTER, BM5357, 1:50; CD8, Proteintech, 66868-1-Ig, 1:200; CD68, Servicebio, GB113150, 1:500). Nucleus were counterstained with DAPI. The autofluorescence was quenched, and photographs were taken under a microscope after mounting.

Selection of cell lines and cell culture conditions

Considering the cell growth characteristics, this experiment used the 143B and U2OS osteosarcoma cell lines, which were obtained from CELLCOOK in Shanghai, China. Cells were identified by STR analysis and confirmed to be free of mycoplasma infection by assays. All cells were cultured in DMEM (Basalmedia, L110kj) containing 10% fetal bovine serum (NEWZERUM, FBS-E500) at 37°C in a cell incubator containing 5% CO_2. Cells in the logarithmic growth phase were used for the experiments.

Lentiviral infection

Lentiviruses for ISG15 overexpression and knockdown were designed and synthesized by GenePharma (Shanghai, China). Lentiviral transfection was carried out according to the manufacturer's protocol. The MOI values selected for 143B and U2OS infections were both 20. Based on relevant literature and preliminary experiments, infected cells were screened with puromycin at a concentration of 1 μg/ml. ISG15 expressions were verified by qRT-PCR and Western blot. More information about ISG15 lentiviruses is provided in Table S1.

Quantitative reverse transcription-PCR

Total RNA was extracted using RNA-easy Isolation Reagent (Vazyme, R701-01) from the cell lines and RNA extraction reagents (Servicebio, G3013-100ml) from tissues, respectively, according to the manufacturer's protocols. cDNA was synthesized according to the manufacturer's instructions. The FastStart Universal SYBR Green Master (Rox) kits were used to determine the expression levels of target genes. PCR amplification was performed using an ABI Prism 7500 rapid thermal cycler, and each sample was normalized to GAPDH as an internal reference gene. The qRT-PCR primers are summarized in Table S2.

Western blotting analysis

Cells from each group were collected and lysed on ice for 30 min by adding RIPA lysis solution (containing PMSF), and cells were fully lysed by an ultrasonic dismantling instrument and centrifuged at 4°C and 12000 rpm for 20 min. The supernatant was placed in an EP tube, and the protein concentration was determined by a BCA protein quantification kit. The gel was made, 20 μg of protein sample per well was added for SDS-PAGE electrophoresis. A 0.22 μm pore size PVDF was used as transfer membrane, which was then blocked in 5% skimmed milk at 280 mA for 90 min. The membrane was

incubated with GAPDH and ISG15 primary antibody (R&D Systems, Monoclonal Mouse IgG2B Clone # 539442) dilution (1:1000) overnight at 4°C, washed 5 times with TBST, 5 min each time, then incubated with secondary antibody dilution for 1 h on a shaker, and again washed 5 times with TBST, 5 min each time. The ECL luminescent solution was developed and exposed with chemiluminescent imager. The grayscale of the bands was analyzed with ImageJ.

Colony formation assay

Three duplicate wells were set in each group, and the cells were evenly seeded in 6-well plates at a cell concentration of 500 cells per well and cultured in a 37°C, 5% CO_2 incubator. The cell growth status was observed every 2-3 days. When visible clones appeared in the culture plate, the culture was terminated, and the supernatant was discarded. Next, the clones were washed twice with PBS, fixed with 2 ml of 4% paraformaldehyde for 20 min. After discard the fixative, we washed the clones twice with PBS, and added 1 ml of 1% crystal violet solution to provide staining for 30 min. Then, the staining solution was slowly washed away with running water. The clones were air-dried, photographed and counted (the number of clones with more than 50 cells).

Wound healing assay

Cells of each group were cultured in 6-well plates to complete confluency to form a monolayer, and a 200 ul pipette tip was used to manually scratch uniformly and forcefully perpendicular to the monolayer in order to create wound areas of approximately the same width and 0 post-wound. After 24 hours or 48 hours, the culture medium was aspirated, and the cells were washed three times with PBS, observed and photographed under an inverted fluorescence microscope.

Transwell assay

In the cell invasion experiments, serum-free cell suspensions from each group were prepared and counted. Then, 300 μL suspension containing 2×10^4-10×10^4 cells was added to the upper chamber which had been pre-coated with Matrigel (Corning, 356234), and 700 μL of DMEM containing 20% serum was added to the lower chamber. After 48 h of incubation at 37°C, the invasive cells adhering to the lower membrane surface were fixed with 4% paraformaldehyde for 30 min and then stained with Giemsa for 3 h at room temperature. Five non-overlapping regions (e.g., upper left, lower left, middle, upper right and lower right) were randomly selected under the microscope to count the number of transmembrane cells and for statistical analysis.

Chemotaxis assays

The chemotaxis of ISG15 to CD8+ T cells and CD68+ cells was carried out using the translucent polycarbonate membrane of 3 μm pore size in 6-well transwell chambers (Corning, 3414). We added 1 ml cells suspension containing 4×10^6 freshly extracted human peripheral lymphocytes into the upper chamber, collected the serum free medium of OE-ISG15 and OE-NC cells cultured for 24 hours with the same initial number of cells, and took 2 ml each as the conditioned medium to add to the lower chamber. The cells were incubated at 37°C and 5% CO_2 for 4 hours. Lower ventricular cells were collected for subsequent FACS analysis.

Flow cytometry

The cell suspension was divided into two equal portions for detecting CD8 and CD68, respectively. The cells were centrifuge at 1000 r for 5 min for precipitation and discarding the supernatant. The cells were moistened with 1 ml of precooled PBS once, centrifuged again for 5 min at 1000 r for precipitation and discarding the supernatant. Then, we added 100 μL buffer and 5 μL of corresponding antibody (CD8, BioLegend, 344703; CD68, BioLegend, 333807) according to the test purpose. The cells were incubated in dark at room temperature for 30 min. Subsequently, the flow cytometer (FACSCalibur) provided by BD Company, USA, was used for computer detection.

Statistical analysis

Bioinformatics statistical analysis and visualization were performed using R (version 3.6.3). Grayscale analysis of Western blot and average fluorescence intensity analysis of immunofluorescence were performed using ImageJ software. Graphical and statistical analyses of wet experiments were performed using GraphPad Prism 8.0 software. The t-test was used for comparison of differences between data with

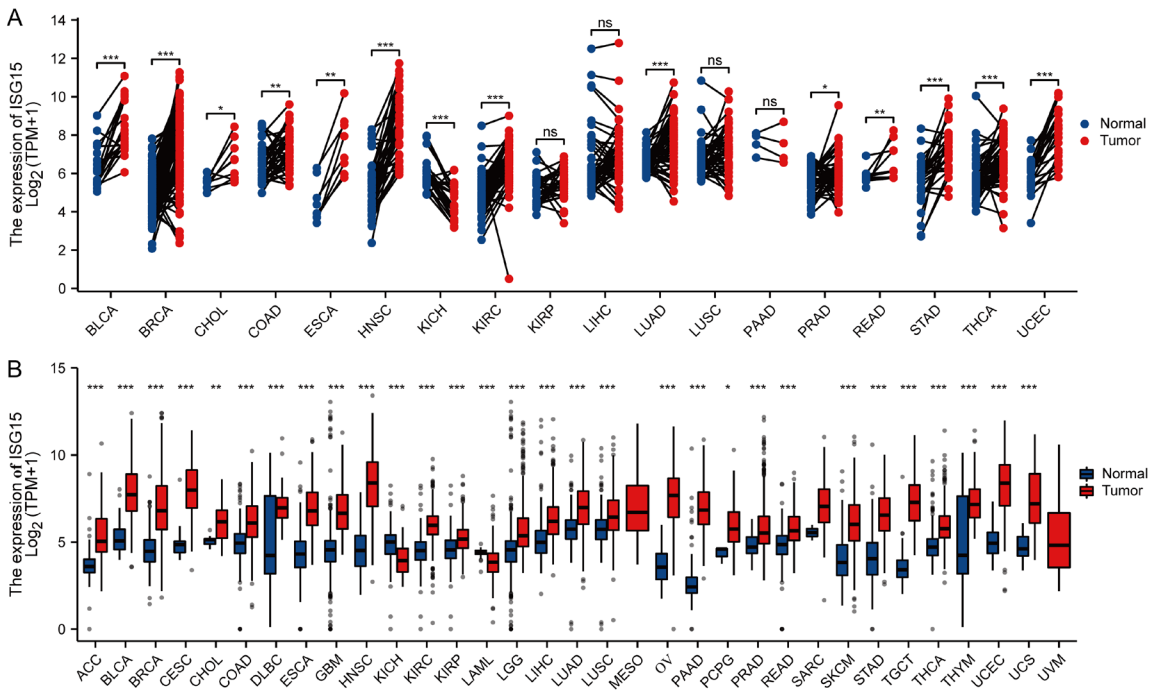

Figure 1. The expression of ISG15 across cancers at a mRNA level in the TCGA and GTEx databases. A. ISG15 expression in normal and tumor tissues in paired samples. B. ISG15 expression in normal and tumor tissues in unpaired samples.

normal distribution. The Wilcoxon signed-rank test was used for data did not meet the normality test. P<0.05 indicates a statistically significant difference. The meaning of symbols and abbreviations are follows: * for P<0.05, ** for P<0.01, *** for P<0.001, **** for P<0.0001, and ns for no significant difference.

Results

Expression of ISG15 across cancers at a mRNA level

RNA-Seq data were downloaded from TCGA to analyze the ISG15 expressions in paired samples of 18 cancers. ISG15 mRNA expressions were higher in tumor tissues than in normal tissues in most cancers, including BLCA, BRCA, CHOL, COAD, ESCA, HNSC, KIRC, LUAD, PRAD, READ, STAD, THCA and UCEC. However, the ISG15 expression was low in KICH (**Figure 1A**). Additionally, data from TCGA and GTEx were also downloaded to analyze the ISG15 expressions in unpaired samples of 33 cancers, which showed that ISG15 was overexpressed in ACC, BLCA, BRCA, CESC, CHOL, COAD, DLBC, ESCA, GBM, HNSC, KIRC, KIRP, LGG, LIHC, LUAD, LUSC, OV, PAAD, PCPG, PRAD, READ, SKCM, STAD, TGCT, THCA, THYM, UCEC and UCS, and lowly expressed in KICH and LAML (**Figure 1B**), similar to the results above.

ISG15 expressions across cancers at a protein level

We compared the IHC results of ISG15 provided by the HPA database, which were in general agreement with those of the ISG15 gene expression analysis by TCGA and GTEx. Normal lung, liver, colon, pancreas, cerebral cortex, stomach, cervical, breast, lymph node and prostate tissues showed negative or moderate staining for ISG15 IHC, and tumor tissues showed moderate or strong staining (**Figure 2A-J**).

Correlation analysis of ISG15 expression and OS in tumor patients

To assess the practical use of ISG15 expressions in predicting the prognosis of tumor patients, we examined the association between ISG15 expression and OS in the TCGA cohort. The KM survival curves demonstrated that higher ISG15 expressions in lung adenocarcinoma (P=0.027), hepatocellular liver cancer

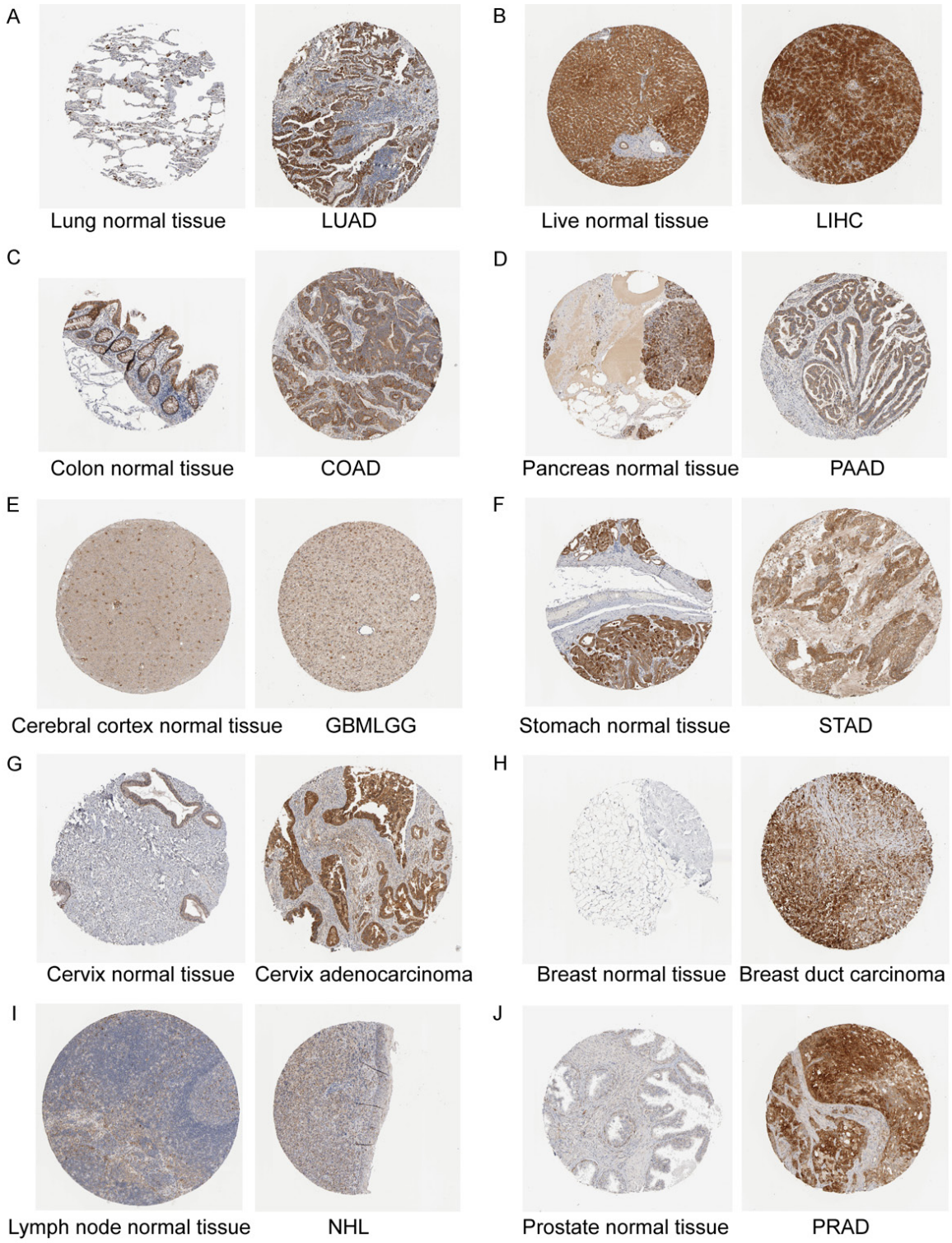

Figure 2. ISG15 expressions across cancers at a protein level in the HPA database. (A) Lung, (B) Live, (C) Colon, (D) Pancreas, (E) Brain, (F) Stomach, (G) Cervix, (H) Breast, (I) Lymph, (J) Prostate.

(P=0.005), colorectal cancer (P=0.014), pancreatic cancer (P=0.01), glioma (P<0.001), uveal melanoma (P=0.005), acute myeloid leukemia (P=0.023), adrenocortical carcinoma (P=0.003) and kidney renal clear cell carcinoma (P<0.001) were significantly associated

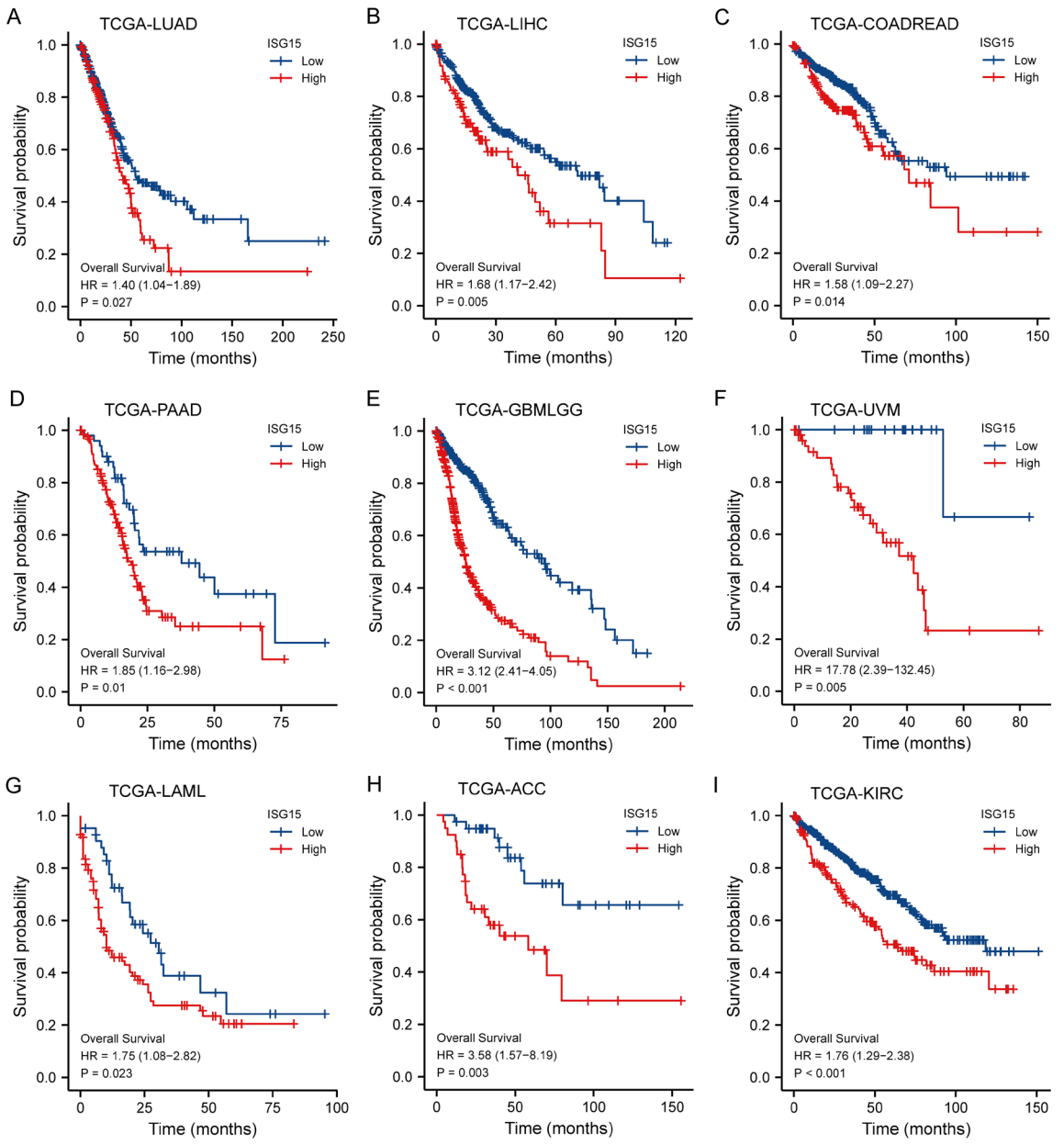

Figure 3. Correlation of ISG15 expression with prognosis of cancer patients. Correlations between ISG15 expression and the OS of (A) LUAD, (B) LIHC, (C) COADREAD, (D) PAAD, (E) GBMLGG, (F) UVM, (G) LAML, (H) ACC, and (I) KIRC were analyzed using the TCGA database.

with shorter OS (**Figure 3A-I**). It is suggested that ISG15 may play a potential cancer-promoting role in these cancers.

Functional and pathway enrichment analysis of ISG15-related genes in sarcoma

To further investigate the function of ISG15, RNA-Seq data of sarcoma were downloaded from the TCGA database and searched for ISG15 expression-related genes. Then, the top 100 most relevant genes to ISG15 were obtained through the "clusterProfile" R package for GO and KEGG enrichment analyses (ggplot2 package [version 3.3.3] for visualization and clusterProfiler package [version 3.14.3] for analysis of the selected data). The data of GO and KEGG analyses showed that most genes were connected with phagosome, Epstein-Barr virus infection, antigen processing and presentation, and type I interferon response (**Figure 4A**). The top 50 genes most positive-

ly associated with ISG15 are presented as a heatmap (**Figure 4B**). The KEGG analysis suggested that antigen processing and presentation, and phagosome might be connected with the oncogenic mechanism of ISG15 (**Figure 4C-E**).

Relationship between ISG15 expression and immune cell infiltration in sarcoma

Previous enrichment analysis showed that ISG15 was mainly associated with antigen processing and presentation, and phagosome in sarcomas. Therefore, we further evaluated whether the ISG15 expression level might be correlated with immune cell infiltration. Spearman's R from ssGSEA (GSVA package built-in algorithm) of the R package GSVA package [version 1.34.0] (Hänzelmann et al., 2013) [13] was used to investigate the potential associations among ISG15 expression levels in sarcoma patient data obtained from the TCGA database and 24 immune cells. A lollipop image is shown in **Figure 5A**, and a trilinear table is shown in **Figure 5B**. The results showed that the ISG15 expressions were related to aDCs, B cells, CD8 T cells, cytotoxic cells, DCs, iDCs, macrophages, neutrophils, NK CD56bright cells, NK CD56dim cells, NK cells, pDCs, T cells, Tems, TFH cells, Th1 cells, Th17 cells, Th2 cells and TReg cells. Further analysis showed that ISG15 was positive correlated with aDC (r=0.516, P<0.001), B cells (r=0.298, P<0.001), CD8 T cells (r=0.207, P<0.001), cytotoxic cells (r=0.411, P<0.001); DC (r=0.309, P<0.001), iDC (r=0.184, P=0.003), macrophages (r=0.311, P<0.001), neutrophils (r=0.368, P<0.001), NK CD56bright cells (r=0.190, P=0.002), NK CD56dim cells (r=0.401, P<0.001), pDC (r=0.143, P=0.021), T cells (r=0.385, P<0.001), Tem (r=0.180, P=0.003), TFH (r=0.171, P=0.005), Th1 cells (r=0.398, P<0.001), Th2 cells (r=0.235, P<0.001), Th17 cells (r=0.176, P=0.004) and TReg (r=0.383, P<0.001), and was negatively correlated only with NK cells (r=-0.159, P=0.010) (**Figure 6**). These results suggests that the high expression of ISG15 may affect the accumulation of immune cells in tumors, and may also be closely related to the changes of immune status in sarcomas.

High ISG15 expressions may be essential for the development of osteosarcoma

First, the expression level of ISG15 in 28 tumor tissues and 19 adjacent/normal tissues were detected by qRT-PCR, which showed that the overall ISG15 expression levels were significantly higher in osteosarcoma primary tissues than in adjacent/normal tissues in 19 paired samples (95% CI: 0.902-15.855, P=0.004) (**Figure 7A**). The same trend was observed in unpaired samples contained 28 tumor tissues and 19 adjacent/normal tissues (95% CI: 0.05-5.186, P=0.032) (**Figure 7B**), suggesting that high ISG15 expressions might be associated with the formation of osteosarcoma. Then, we defined cases with ISG15 expression above the median as ISG15 high expression ($2^{-\Delta\Delta CT}$> 0.663962829), and conversely as low expression ($2^{-\Delta\Delta CT}$≤0.663962829). The correlation between ISG15 and clinical features in osteosarcoma was analyzed. The results in **Table 1** suggested that ISG15 expression was associated with lung metastasis (P=0.021). Protein expressions of ISG15 were measured by IHC in 28 tumor tissues, 19 adjacent/normal tissues and 5 lung metastatic tissues (**Figure 7C**). The overall trend showed that the staining intensities of ISG15 were higher in osteosarcoma primary tissues with lung metastasis than in osteosarcoma primary tissues without lung metastasis. Adjacent/normal tissues showed mild staining of ISG15, and nonspecific staining was not excluded. It should be noted that ISG15 staining was strongly positive in 5 cases of lung metastatic lesions. These results indicate that the expression of ISG15 is upregulated in osteosarcoma and correlated with the pulmonary metastasis of osteosarcoma.

ISG15 knockdown significantly inhibits the proliferation, migration and invasive ability of 143B and U2OS osteosarcoma cells in vitro

The qRT-PCR and Western blot results are shown in **Figure 8A**, **8B**. In 143B and U2OS cells, the expression levels of ISG15 were significantly increased in the OE-ISG15 group compared with that of the OE-NC group and knocked down in the sh-ISG15 group compared with that of the sh-NC group (P<0.05), indicating that the stable transgenic cells were successfully constructed. Next, we further demonstrated the oncogenic role of ISG15 in osteosarcoma. As shown in **Figure 8C**, ISG15 overexpression significantly promoted the proliferative ability of 143B and U2OS cells compared with those of the OE-NC group, and ISG15 knockdown significantly inhibited the proliferation ability of 143B and U2OS cells compared with

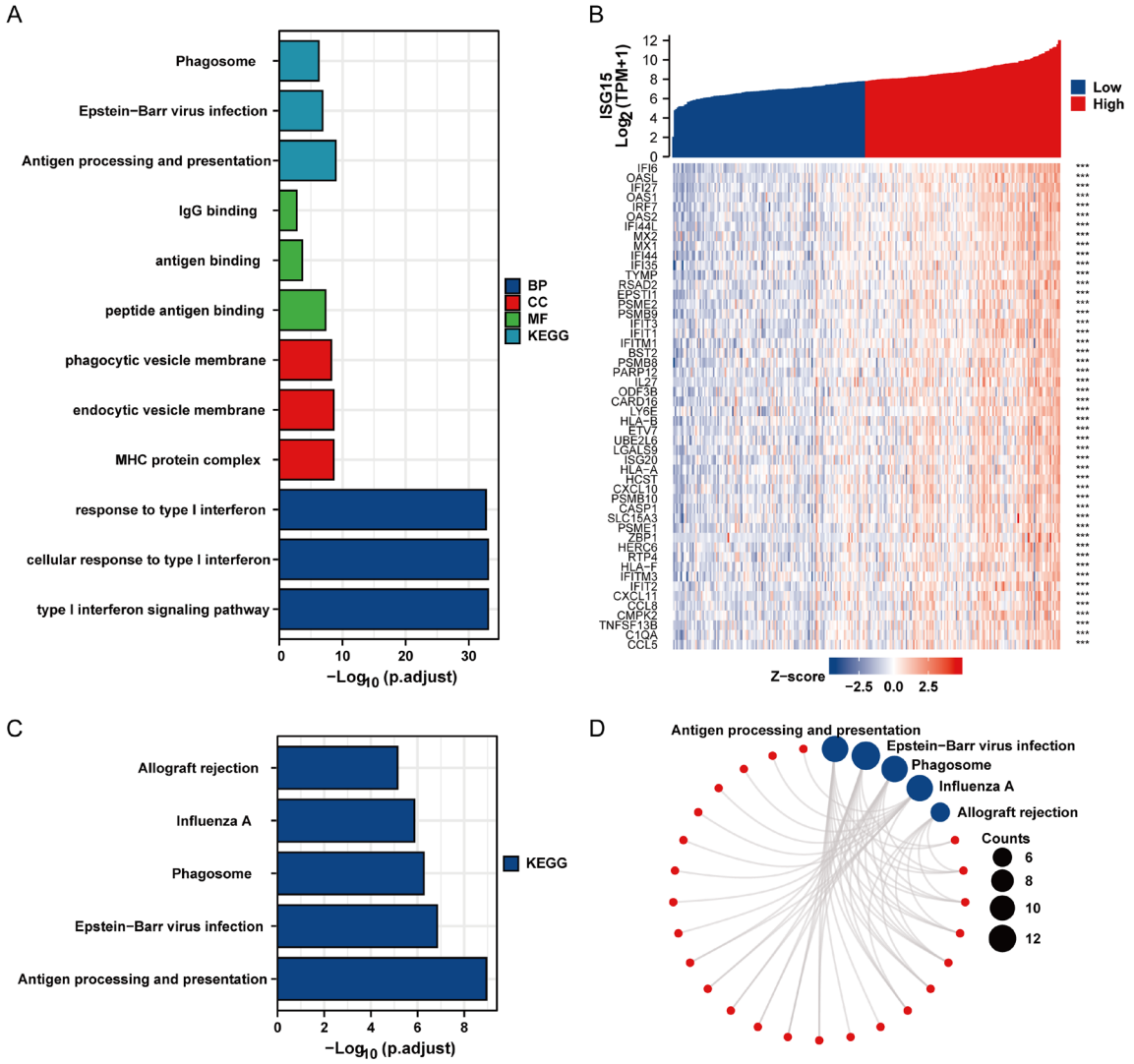

E

Ontology	ID	Description	GeneRatio	BgRatio	pvalue	p.adjust	qvalue
KEGG	hsa04612	Antigen processing and presentation	11/62	78/8076	1.13e-11	1.12e-09	7.01e-10
KEGG	hsa05169	Epstein-Barr virus infection	13/62	202/8076	2.89e-09	1.43e-07	8.96e-08
KEGG	hsa04145	Phagosome	11/62	152/8076	1.63e-08	5.37e-07	3.37e-07
KEGG	hsa05164	Influenza A	11/62	171/8076	5.55e-08	1.37e-06	8.61e-07
KEGG	hsa05330	Allograft rejection	6/62	38/8076	3.65e-07	7.22e-06	4.53e-06

Figure 4. Function and pathway enrichment analysis of ISG15 in SARC. (A) Significant Gene Ontology terms (including BP, CC and MF) and KEGG analyses of the top 100 genes most positively associated with ISG15. (B) Heatmap of the top 50 genes most positively associated with ISG15. Histogram (C), ring type visualization network (D) and three-line watch (E) were used to present the significant KEGG pathway of the top 100 genes most positively associated with ISG15.

those in the sh-NC group (P<0.05). Furthermore, as shown in **Figure 8D**, **8E**, ISG15 overexpression significantly promoted the migration and invasion of 143B and U2OS cells compared with those of the OE-NC group, and ISG15 knockdown significantly inhibited the migration

A

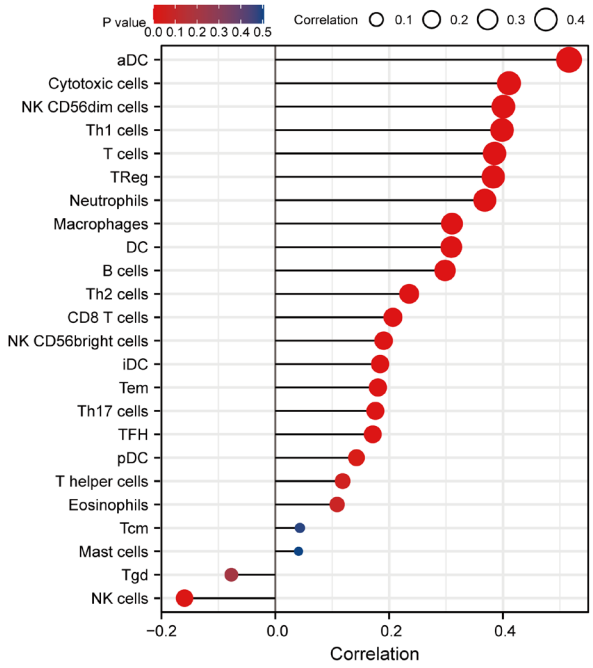

B

Molecular	Immune Cells	P value (Spearman)
ISG15	aDC	<0.001
ISG15	B cells	<0.001
ISG15	CD8 T cells	<0.001
ISG15	Cytotoxic cells	<0.001
ISG15	DC	<0.001
ISG15	iDC	0.003
ISG15	Macrophages	<0.001
ISG15	Neutrophils	<0.001
ISG15	NK CD56bright cells	0.002
ISG15	NK CD56dim cells	<0.001
ISG15	NK cells	0.010
ISG15	pDC	0.021
ISG15	T cells	<0.001
ISG15	Tem	0.003
ISG15	TFH	0.005
ISG15	Th1 cells	<0.001
ISG15	Th17 cells	0.004
ISG15	Th2 cells	<0.001
ISG15	TReg	<0.001

Figure 5. Lollipop image (A) and three-line table (B) showing the relationship between ISG15 and immune cell infiltration.

and invasion of 143B and U2OS cells (P<0.05). These data suggest that ISG15 expressions are positively correlated with osteosarcoma cell proliferation, migration and invasion abilities in vitro.

Overexpression of ISG15 can recruit CD68+ immune cells and weaken the chemotaxis of CD8+ T cells

The correlations between ISG15 levels and CD8+ T cells/CD68+ cells in osteosarcoma tissue in the ISG15 high expression and low expression groups were detected by the double-labeled immunofluorescence. Representative images showed that the expression of ISG15 were negatively associated with the number of infiltrating CD8+ T cells and positively associated with CD68+ cells (**Figure 9A**). We further confirmed in vitro by chemotaxis assays and flow cytometry that overexpression of ISG15 induced chemotaxis of CD68+ cells (P<0.0001) but reduced the chemotaxis of CD8+ T cells (P<0.0001) (**Figure 9B**). The results above suggest that ISG15 may participated in the occurrence and development of osteosarcoma by affecting immune cell infiltration levels.

Discussion

ISG15 is known to be involved in the occurrence and development of tumors and is closely related to tumor prognosis [15-17]. Kariri et al. have provided evidence that increasing ISG15 at transcriptomic and proteomic levels was strongly associated with shorter specific survival times in patients with invasive breast cancer [18]. It has also been shown that ISG15 is overexpressed in nasopharyngeal carcinoma (NPC) tissue samples and cell lines and is proven to be linked to shorter OS and disease-free survival and higher local recurrence rate [19]. In NPC cells, ISG15 overexpression promoted cancer stem cell phenotypes, including increased colony and tumorsphere-forming capacity, pluripotency-related gene expression, and tumorigenicity in vivo, with protumorigenic functions. Its overexpression is a poor prognostic factor a potential therapeutic target for NPC. The ISG15 expressions across cancers in the TCGA and GTEX databases were analyzed in our study, and we further evaluated the relationship between ISG15 expressions and patient prognoses by using TCGA clinical survival data. The results were consistent with most of previous studies. ISG15 was more high-

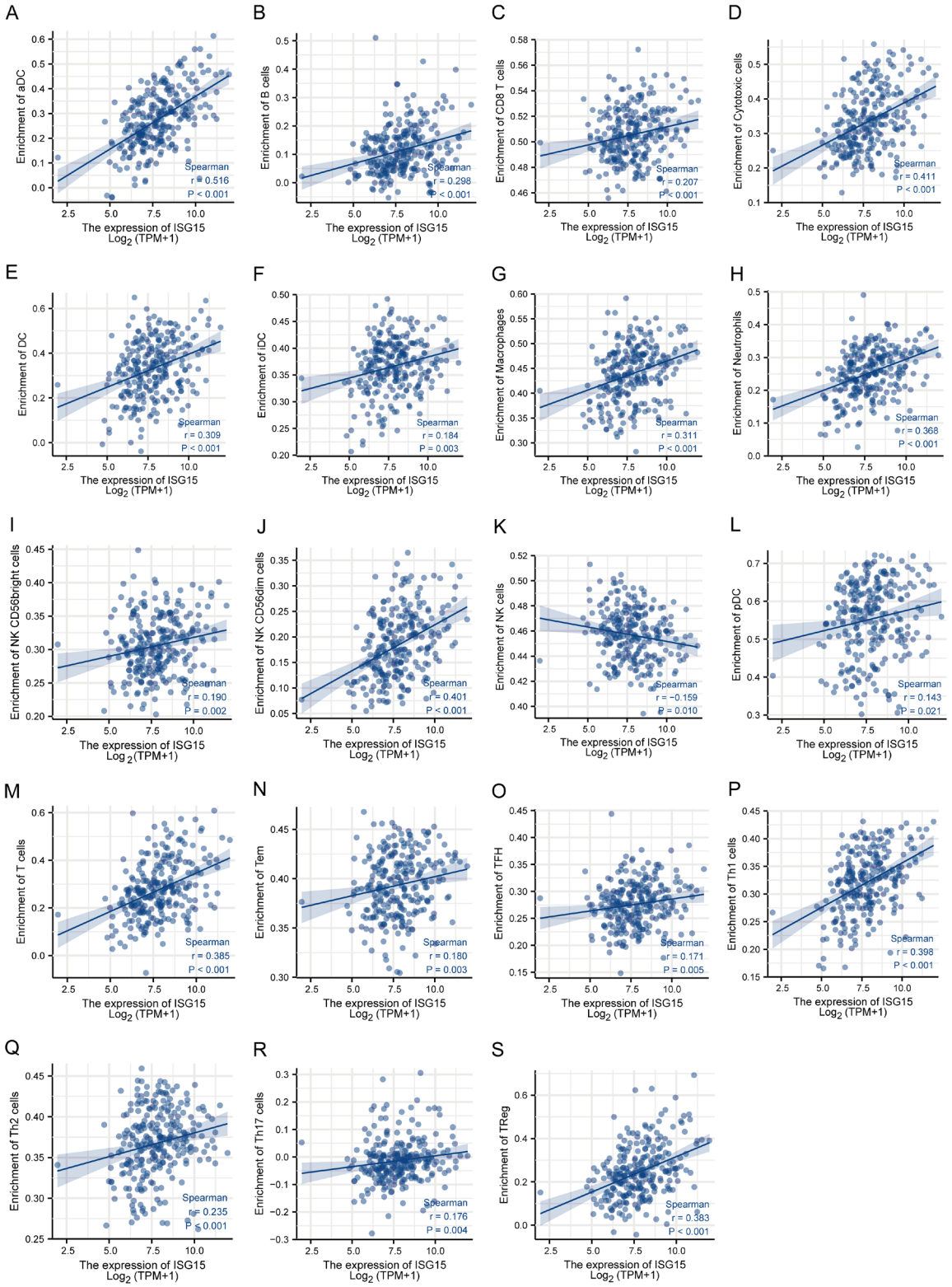

Figure 6. Scatter plot showing the correlation between the expression of ISG15 and immune cell. (A) aDC, (B) B cells, (C) CD8 T cells, (D) Cytotoxic cells, (E) DC, (F) iDC, (G) Macrophages, (H) Neutrophils, (I) NK CD56bright cells, (J) NK CD56dim cells, (K) NK cells, (L) pDC, (M) T cells, (N) Tem, (O) TFH, (P) Th1 cells, (Q) Th2 cells, (R) Th17 cells and (S) TReg.

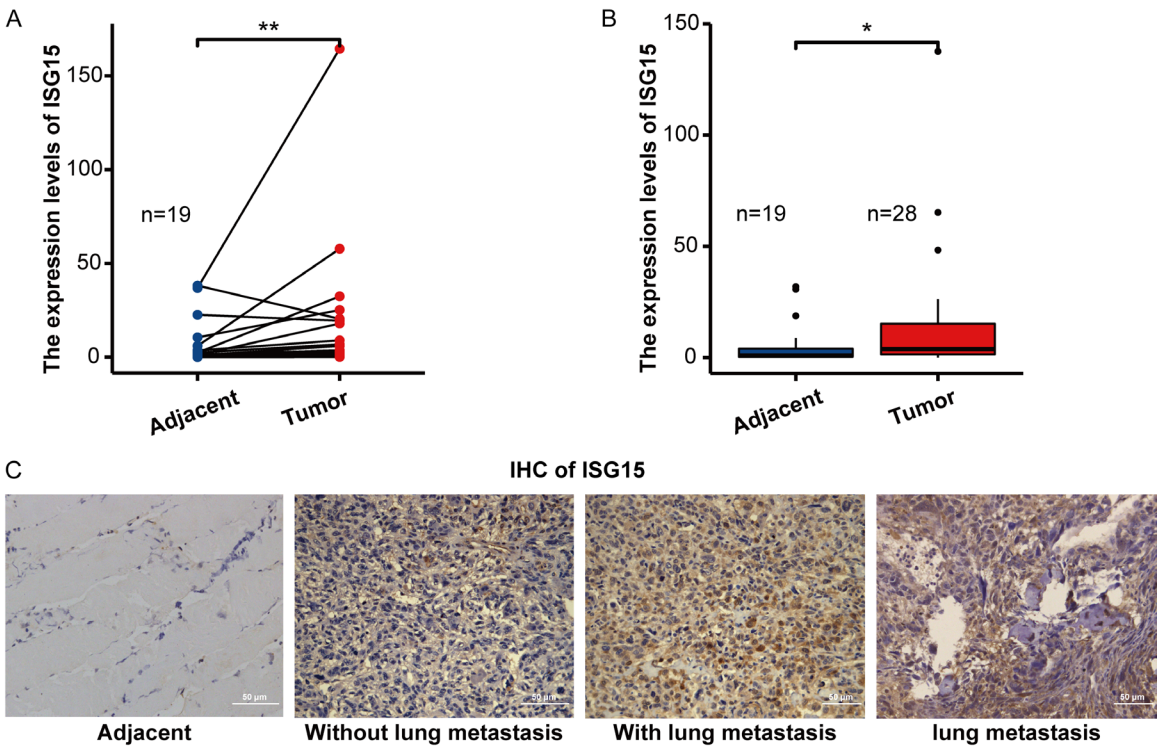

Figure 7. Expression of ISG15 in clinical samples of osteosarcoma. A. The mRNA levels of ISG15 in 19 paired samples of adjacent/normal tissues and osteosarcoma tissues were determined by qRT-PCR. B. The mRNA levels of ISG15 in unpaired samples (28 tumor tissues and 19 adjacent/normal tissues) were determined by qRT-PCR. C. ISG15 expression in adjacent/normal tissue, osteosarcoma tissue with or without lung metastasis and in pulmonary metastatic lesions were determined by immunohistochemistry (200×).

Table 1. The correlation between ISG15 and clinical features of osteosarcoma

Characteristic	High expression of ISG15	Low expression of ISG15	*p*
n	14	14	
Gender, n (%)			1.000
Female	6 (21.4%)	6 (21.4%)	
Male	8 (28.6%)	8 (28.6%)	
Age, n (%)			1.000
<18	8 (28.6%)	8 (28.6%)	
≥18	6 (21.4%)	6 (21.4%)	
T stage, n (%)			1.000
T1	7 (25%)	6 (21.4%)	
T2	7 (25%)	8 (28.6%)	
Tumor region, n (%)			0.871
Distal femur	6 (21.4%)	8 (28.6%)	
Other	2 (7.1%)	1 (3.6%)	
Proximal humerus	1 (3.6%)	1 (3.6%)	
Proximal tibia	5 (17.9%)	4 (14.3%)	
Lung metastasis, n (%)			0.021
No	3 (10.7%)	10 (35.7%)	
Yes	11 (39.3%)	4 (14.3%)	

ly expressed in most tumor tissues than in normal/adjacent tissues, and patients with high expressions tended to have poor prognosis. Based on previous studies, ISG15 was overexpressed in various tumors and had been identified as a prognostic factor, while few studies have explored the association of ISG15 expression with osteosarcoma. So, it is necessary to explore the relationship between ISG15 expression and the occurrence and development of osteosarcoma.

Through studies of clinical samples, we found that at the mRNA level, the overall expression levels of ISG15 in primary osteosarcoma tissue were significantly higher than those in adjacent/normal tissues. IHC images showed that the protein expression level of ISG15 in primary osteosarcoma samples with lung metastasis was significantly higher than that in those

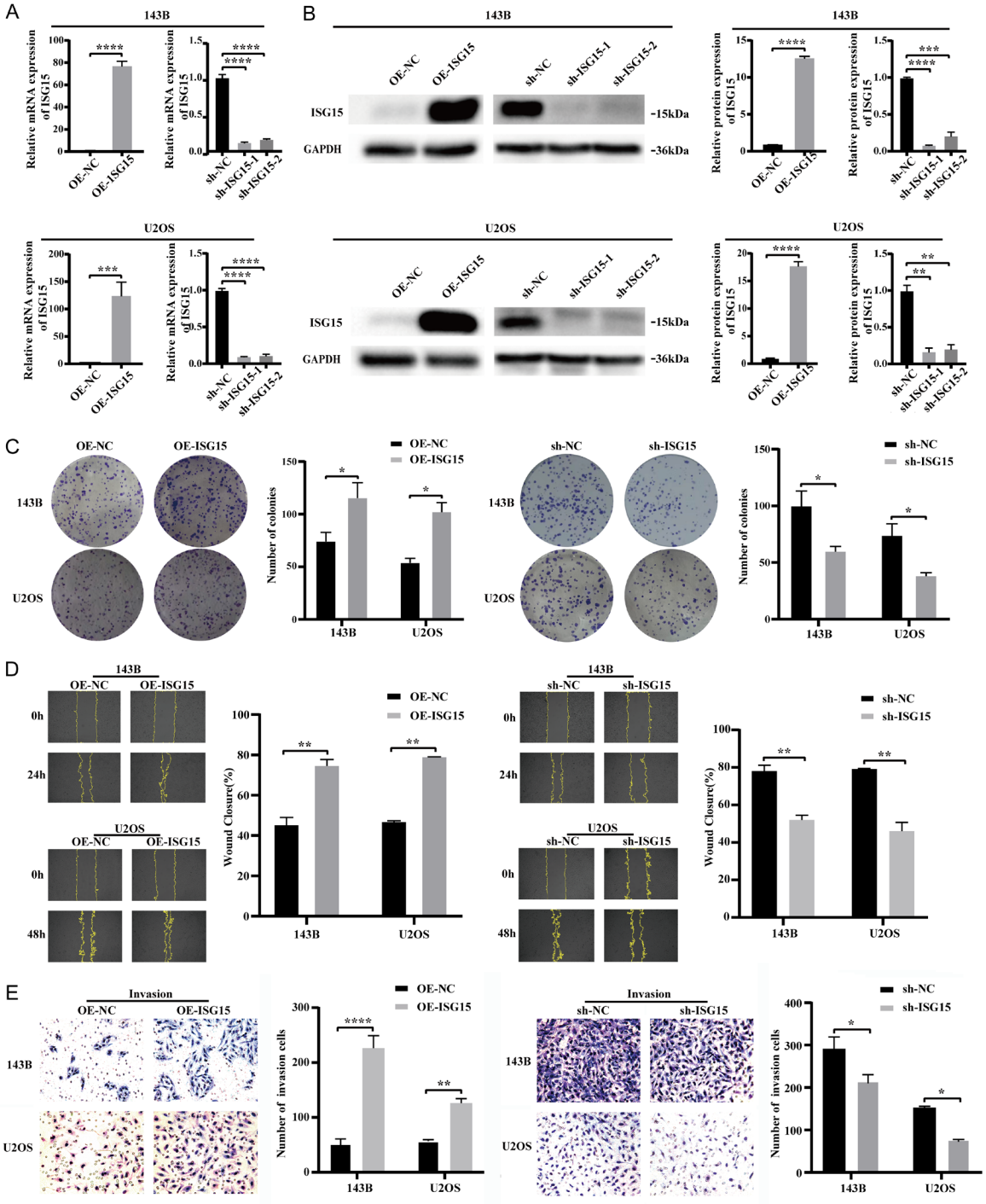

Figure 8. Effects of ISG15 expression on proliferation, migration and invasion of osteosarcoma cells. A. 143B and U2OS cells were transfected with lentivirus of OE-ISG15 or sh-ISG15, and the level of ISG15 was assessed by qRT-PCR. B. 143B and U2OS cells were transfected with lentivirus of OE-ISG15 or sh-ISG15, and the level of ISG15 was assessed by Western blot. C. The proliferation ability of osteosarcoma cells was examined by colony formation assay. D. The migration abilities of osteosarcoma cells were detected by wound healing assay. E. The invasion abilities of osteosarcoma cells were detected by transwell assay.

without lung metastasis, suggesting that high expression of ISG15 might play a crucial role in the occurrence of lung metastasis in osteosarcoma. We further validated that at the cellular level, high ISG15 expressions significantly promoted the proliferation, migration and invasion

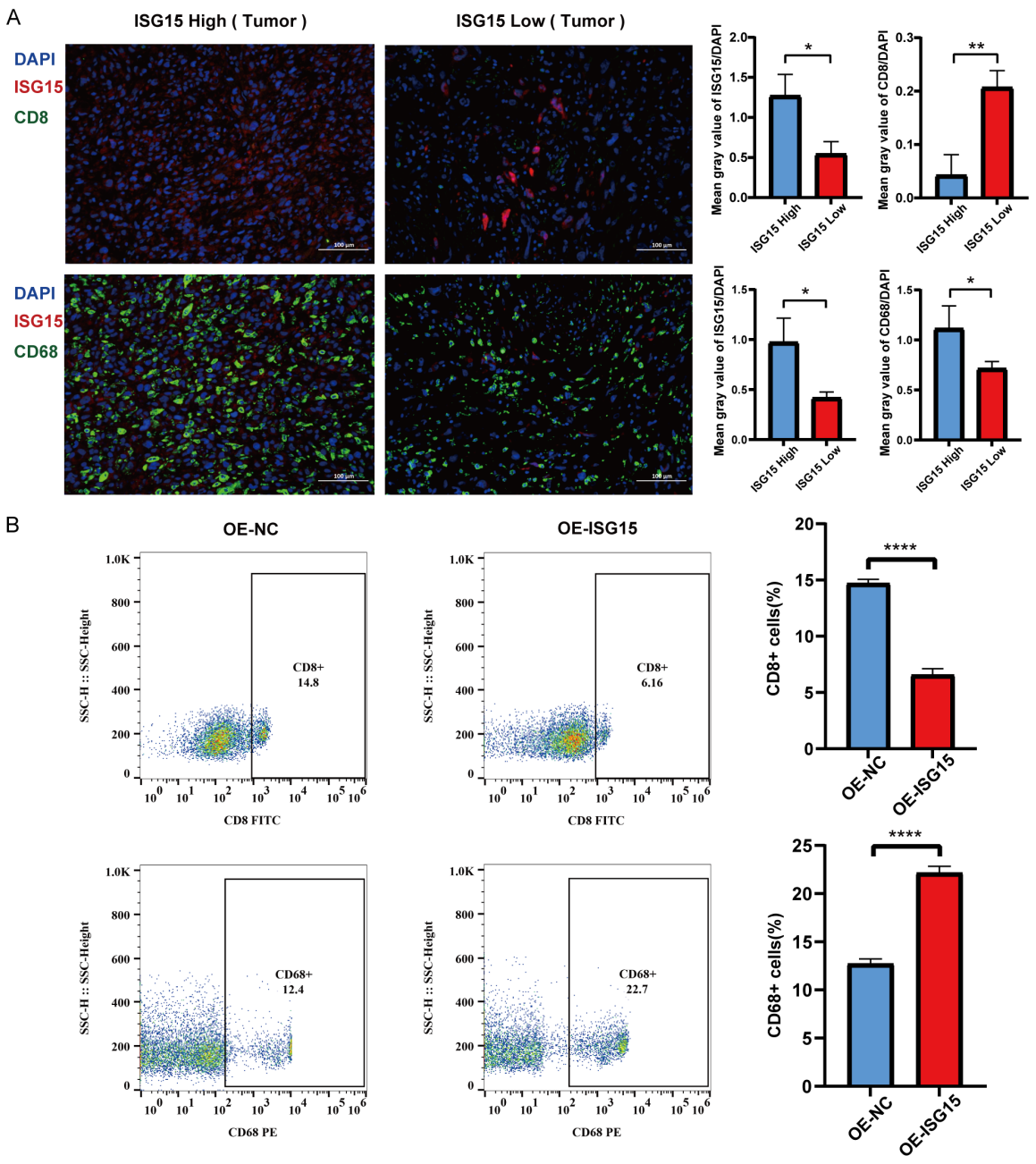

Figure 9. The correlation between the ISG15 level and the infiltration of CD8+ T cells/CD68+ cells in osteosarcoma. A. The expression of ISG15 were negatively associated with the number of infiltrating CD8+ T cells and positively associated with CD68+ cells, as determined by double-labeled immunofluorescence (200×). B. Chemotaxis assays and flow cytometry showed that the overexpression of ISG15 induced chemotaxis of CD68+ cells ($P<0.0001$) but reduced the chemotaxis of CD8+ T cells ($P<0.0001$).

of 143B and U2OS osteosarcoma cells. These results suggested that an oncogene role of ISG15 in osteosarcoma is similar to cell-level studies of glioma, nasopharyngeal carcinoma, breast cancer, colorectal cancer, lung cancer and bladder cancer. Based on the above research results, we can reasonably speculate that ISG15 has broad application prospects in the diagnosis and prognosis evaluation of osteosarcoma. The underlying mechanism and feasibility of ISG15 as a molecular biomarker for osteosarcoma are also worthy of further investigation.

The TME is a complex integrated system and mainly composed of tumor cells and their sur-

rounding immune and inflammatory cells, tumor-associated fibroblasts, nearby interstitial tissues, microvessels, various cytokines and chemokines [20, 21]. It can be divided into an immune microenvironment dominated by immune cells and a nonimmune microenvironment dominated by fibroblasts. Tumor cells can interact with surrounding cells through the circulatory and lymphatic systems to influence cancer development and progression [22]. Accumulating evidence implicates ISG15 and ISGylation participate in a variety of key cellular processes [9, 23], including immune regulation, autophagy, protein translation, exosome secretion and DNA repair. The effects of ISG15 on tumor development are closely related to the TME. ISG15 is highly expressed in most tumors, which may be connected with immune cell infiltration into the tumor stroma, which leads to increased ISG15 expression in tumor cells because these cells are major sources of interferon α and β [18]. Tumor-associated macrophages (TAMs) secrete the IFN-stimulating factor, ISG15, which can enhance the phenotype of cancer stem cells (CSCs) in pancreatic ductal adenocarcinoma cells (PDACs) in vitro and in vivo [24]. Enhancement of the self-renewal, invasion and tumorigenicity of CSCs suggests that ISG15 may play a tumor-promoting role through immune regulation. ISG15 has been reported to play a crucial role in TEM by enhancing T cells, B cells and epithelial cell line cytokines [12]. Both IFN induction and immune cell activation are important mediators of cancer immunogenicity and are associated with the expression of ISG15. In this study, the results of gene function and pathway enrichment analyses of ISG15 in sarcoma also showed that most genes related to ISG15 were related to phagosomes, EB virus infection, antigen processing and presentation, and type I interferon reaction. Antigen processing and presentation are possible carcinogenic mechanisms of ISG15.

It has been shown that free ISG15 secreted by melanoma cells modulates the phenotype of tumor-infiltrating dendritic cells (DCs) by stimulating the expression of E-cadherin, which is an adhesion molecule that impairs DC motility, leading to tumor escape [9]. In addition, ISG15, which can respond to type I interferons, has been shown to be secreted by TAMs produced by PDACs, accelerating the tumorigenesis of CSCs [24]. These results suggest that ISG15 has a tumor-promoting role in cancer immunogenicity.

The relationship between ISG15 expression and immune cell infiltration in sarcoma was analyzed by bioinformatics analysis, which suggested that the high expression of ISG15 might affect the accumulation of immune cells in tumors, and might be closely related to the changes of immune status in sarcomas. In endometrial carcinoma with a high level of ISG15, it can be found that the expression of T cell inhibitor (such as PD-L1) is higher, while CD8+ T cells are significantly reduced, and the killing activity is inhibited, making tumor cells have a stronger immune escape ability [25]. Chen et al. showed that ISG15 secreted by tumor cells could promote tumor cell migration and immunosuppression by inducing the M2-like phenotype of macrophages [26]. Additionally, it has emerged that tumor progression is affected by the composition of the TME and is controlled by the host immune system [27]. Therefore, the components of the TME and immune system biomarkers are truly important for cancer detection, prognosis assessment, prediction of treatment response. The expression of ISG15 were negatively associated with the number of infiltrating CD8+ T cells and positively associated with CD68+ cells, as determined by double-labeled immunofluorescence in our study. Chemotaxis assays and flow cytometry showed that overexpression of ISG15 induced chemotaxis of CD68+ cells, but reduced the chemotaxis of CD8+ T cells. CD8+ T cells usually differentiate into cytotoxic T cells after activation, and cytotoxic T cells will then penetrate into the core or invasion site of the tumor and play an important role in killing cancer cells [28]. CD8+ T cells activated by tumor immunotherapy mainly eliminate tumors by inducing cell death through perforin granzyme and Fas ligand pathways [29]. After comprehensive analysis, we speculated that ISG15 regulates the occurrence and development of osteosarcoma by affecting the level of immune cell infiltration.

Conclusions

In conclusion, we demonstrated that ISG15 expressions were upregulated in osteosarcoma tumor tissue compared to adjacent/normal tissue, and were higher in primary tissue with lung metastasis than those without lung metasta-

sis. Further in vitro cytological experiments proved that ISG15 overexpression could significantly promote the proliferation, migration and invasion of osteosarcoma cells, suggesting that ISG15 might be significantly relevant to the occurrence and metastasis of osteosarcoma. In addition, ISG15 might also participate in the occurrence and development of osteosarcoma by affecting immune cell infiltration levels. The specific mechanism of action remains to be further studied.

Thus, our findings reveal the role of ISG15 in osteosarcoma and identify ISG15 as a promising prognostic biomarker for osteosarcoma therapy.

Acknowledgements

This research was supported by grants from the National Natural Science Foundation of China (No. 81760520), Applied Basic Research Key Project of Yunnan (No. 202101AS070004), and Joint Special Funds for the Department of Science and Technology of Yunnan Province Kunming Medical University (No. 202101AY070001-173, No. 202001AY070001-073 and No. 2019FE001(-238)).

Disclosure of conflict of interest

The authors declare that the research was conducted in the absence of any commercial or financial relationships that could be construed as a potential conflict of interest.

Address correspondence to: Dr. Lin Xie, Department of Gastrointestinal Oncology, The Third Affiliated Hospital of Kunming Medical University (Yunnan Cancer Hospital, Yunnan Cancer Center), No. 519, Kunzhou Road, Xishan District, Kunming 650118, Yunnan, China. Tel: +86-0871-68178612; E-mail: xielin@kmmu.edu.cn

References

[1] Shi L, Xie C, Zhu J and Chen X. Downregulation of serum miR-194 predicts poor prognosis in osteosarcoma patients. Ann Diagn Pathol 2020; 46: 151488.

[2] Wang B and Sun Y. SELPLG expression was potentially correlated with metastasis and prognosis of osteosarcoma. Pathol Oncol Res 2022; 28: 1610047.

[3] Chen C, Mao X, Cheng C, Jiao Y, Zhou Y, Ren T, Wu Z, Lv Z, Sun X and Guo W. MiR-135a reduces osteosarcoma pulmonary metastasis by targeting both BMI1 and KLF4. Front Oncol 2021; 11: 620295.

[4] Zhang C, Zheng JH, Lin ZH, Lv HY, Ye ZM, Chen YP and Zhang XY. Profiles of immune cell infiltration and immune-related genes in the tumor microenvironment of osteosarcoma. Aging (Albany NY) 2020; 12: 3486-501.

[5] Huang H, Han Y, Chen Z, Pan X, Yuan P, Zhao X, Zhu H, Wang J, Sun X and Shi P. ML264 inhibits osteosarcoma growth and metastasis via inhibition of JAK2/STAT3 and WNT/beta-catenin signalling pathways. J Cell Mol Med 2020; 24: 5652-64.

[6] Glover J, Krailo M, Tello T, Marina N, Janeway K, Barkauskas D, Fan TM, Gorlick R and Khanna C; COG Osteosarcoma Biology Group. A summary of the osteosarcoma banking efforts: a report from the Children'S Oncology Group and the QuadW Foundation. Pediatr Blood Cancer 2015; 62: 450-5.

[7] Wang X, Qin G, Liang X, Wang W, Wang Z, Liao D, Zhong L, Zhang R, Zeng YX, Wu Y and Kang T. Targeting the CK1α/CBX4 axis for metastasis in osteosarcoma. Nat Commun 2020; 11: 1141.

[8] Mirzalieva O, Juncker M, Schwartzenburg J and Desai S. ISG15 and ISGylation in human diseases. Cells 2022; 11: 538.

[9] Han HG, Moon HW and Jeon YJ. ISG15 in cancer: beyond ubiquitin-like protein. Cancer Lett 2018; 438: 52-62.

[10] Yang YH, Zhang Y, Qu X, Xia JF, Li DQ, Li XJ, Wang Y, He ZW, Li S, Zhou YH, Xie L and Yang ZZ. Identification of differentially expressed genes in the development of osteosarcoma using RNA-seq. Oncotarget 2016; 7: 87194-87205.

[11] DuFort CC, DelGorno KE and Hingorani SR. Mounting pressure in the microenvironment: fluids, solids, and cells in pancreatic ductal adenocarcinoma. Gastroenterology 2016; 150: 1545-1557.

[12] D'Cunha J, Knight E Jr, Haas AL, Truitt RL and Borden EC. Immunoregulatory properties of ISG15, an interferon-induced cytokine. Proc Natl Acad Sci U S A 1996; 93: 211-215.

[13] Hänzelmann S, Castelo R and Guinney J. GSVA: gene set variation analysis for microarray and RNA-Seq data. BMC Bioinformatics 2013; 14: 7.

[14] Bindea G, Mlecnik B, Tosolini M, Kirilovsky A, Waldner M, Obenauf AC, Angell H, Fredriksen T, Lafontaine L, Berger A, Bruneval P, Fridman WH, Becker C, Pagès F, Speicher MR, Trajanoski Z and Galon J. Spatiotemporal dynamics of intratumoral immune cells reveal the immune landscape in human cancer. Immunity 2013; 39: 782-795.

[15] Forys JT, Kuzmicki CE, Saporita AJ, Winkeler CL, Maggi LB Jr and Weber JD. ARF and p53 coordinate tumor suppression of an oncogenic IFN-β-STAT1-ISG15 signaling axis. Cell Rep 2014; 7: 514-526.
[16] Bektas N, Noetzel E, Veeck J, Press MF, Kristiansen G, Naami A, Hartmann A, Dimmler A, Beckmann MW, Knüchel R, Fasching PA and Dahl E. The ubiquitin-like molecule interferon-stimulated gene 15 (ISG15) is a potential prognostic marker in human breast cancer. Breast Cancer Res 2008; 10: R58.
[17] Qiu XX, Hong Y, Yang DR, Xia M, Zhu HZ, Li QL, Xie HL, Wu QF, Liu C and Zuo CH. ISG15 as a novel prognostic biomarker for hepatitis B virus-related hepatocellular carcinoma. Int J Clin Exp Med 2015; 8: 17140-50.
[18] Kariri YA, Alsaleem M, Joseph C, Alsaeed S, Aljohani A, Shiino S, Mohammed OJ, Toss MS, Green AR and Rakha EA. The prognostic signifcance of interferon-stimulated gene 15 (ISG15) in invasive breast cancer. Breast Cancer Res Treat 2021; 185: 293-305.
[19] Chen RH, Du Y, Han P, Wang HB, Liang FY, Feng GK, Zhou AJ, Cai MY, Zhong Q, Zeng MS and Huang XM. ISG15 predicts poor prognosis and promotes cancer stem cell phenotype in nasopharyngeal carcinoma. Oncotarget 2016; 7: 16910-22.
[20] Arneth B. Tumor microenvironment. Medicina (Kaunas) 2019; 56: 15.
[21] LeBleu VS. Imaging the tumor microenvironment. Cancer J 2015; 21: 174-178.
[22] Fong EL, Harrington DA, Farach-Carson MC and Yu H. Heralding a new paradigm in 3D tumor modeling. Biomaterials 2016; 108: 197-213.
[23] Dzimianski JV, Scholte FEM, Bergeron É and Pegan SD. ISG15: it's complicated. J Mol Biol 2019; 431: 4203-4216.
[24] Sainz B Jr, Martín B, Tatari M, Heeschen C and Guerra S. ISG15 is a critical microenvironmental factor for pancreatic cancer stem cells. Cancer Res 2014; 74: 7309-7320.
[25] Zhao XW, Wang JJ, Wang YJ, Zhang MM, Zhao W, Zhang H and Zhao LM. Interferon-stimulated gene 15 promotes progression of endometrial carcinoma and weakens antitumor immune response. Oncol Rep 2022; 47: 110.
[26] Chen RH, Xiao ZW, Yan XQ, Han P, Liang FY, Wang JY, Yu ST, Zhang TZ, Chen SQ, Zhong Q and Huang XM. Tumor cell-secreted ISG15 promotes tumor cell migration and immune suppression by inducing the macrophage M2-like phenotype. Front Immunol 2020; 11: 594775.
[27] Watnick RS. The role of the tumor microenvironment in regulating angiogenesis. Cold Spring Harb Perspect Med 2012; 2: a006676.
[28] Farhood B, Najafi M and Mortezaee K. CD8+ cytotoxic T lymphocytes in cancer immunotherapy: a review. J Cell Physiol 2019; 234: 8509-8521.
[29] Zhang L, Zhang W, Li ZY, Lin SM, Zheng TS, Hao BJ, Hou YQ, Zhang YF, Wang K ,Qin CJ, Yue LD, Jin J, Li M and Fan LH. Mitochondria dysfunction in CD8+ T cells as an important contributing factor for cancer development and a potential target for cancer treatment: a review. J Exp Clin Cancer Res 2022; 41: 227.

Table S1. The information of lentiviruses

Gene Name	Sequence (5'-3')
ISG15-shRNA-NC	TTCTCCGAACGTGTCACGT
ISG15-shRNA-1	GCACCGTGTTCATGAATCTGC
ISG15-shRNA-2	GCATCCTGGTGAGGAATAACA
ISG15-OE-NC	—
ISG15-OE	ATGGGCTGGGACCTGACGGTGAAGATGCTGGCGGGCAACGAATTCCAGGTGTCCCTGAGCAGCTCCATGTCGGTGTCAGAGCTGAAGGCGCAGATCACCCAGAAGATCGGCGTGCACGCCTTCCAGCAGCGTCTGGCTGTCCACCCGAGCGGTGTGGCGCTGCAGGACAGGGTCCCCCTTGCCAGCCAGGGCCTGGGCCCCGGCAGCACGGTCCTGCTGGTGGTGGACAAATGCGACGAACCTCTGAGCATCCTGGTGAGGAATAACAAGGGCCGCAGCAGCACCTACGAGGTACGGCTGACGCAGACCGTGGCCCACCTGAAGCAGCAAGTGAGCGGGCTGGAGGGTGTGCAGGACGACCTGTTCTGGCTGACCTTCGAGGGGAAGCCCCTGGAGGACCAGCTCCCGCTGGGGGAGTACGGCCTCAAGCCCCTGAGCACCGTGTTCATGAATCTGCGCCTGCGGGGAGGCGGCACAGAGCCTGGCGGGCGGAGCTAA

Table S2. The sequence of primers

Gene Name	Primer sequence (5'-3')
GAPDH	Forward: TGCACCACCAACTGCTTAGC
	Reverse: GGCATGGACTGTGGTCATGAG
ISG15	Forward: CGCAGATCACCCAGAAGATCG
	Reverse: TTGGTCGCATTTGTCCACCA